Observation of anomalous magnetism in the low-temperature monoclinic phase of single-crystalline $PrAlO_3$ perovskite

M. Wencka,[1,*] S. Vrtnik,[1] M. Jagodič,[2] Z. Jagličić,[2] S. Turczynski,[3] D. A. Pawlak,[3] and J. Dolinšek[1]
[1]*J. Stefan Institute, University of Ljubljana, Jamova 39, SI-1000 Ljubljana, Slovenia*
[2]*Institute of Mathematics, Physics and Mechanics, University of Ljubljana, Jadranska 19, SI-1000 Ljubljana, Slovenia*
[3]*Institute of Electronic Materials Technology, ul. Wolczynska 133, PL-01 919 Warsaw, Poland*
(Received 9 September 2009; published 8 December 2009)

We have investigated unusual magnetism of the $PrAlO_3$ perovskite system by performing measurements of the magnetization, magnetic susceptibility, and ^{27}Al NMR spectra on single crystals, prepared by the Czochralski method. Two kinds of samples were investigated, an as-grown crystal containing a mixture of Pr^{3+} and Pr^{4+} ions in the approximate ratio 4:1 and a crystal annealed in a reducing H_2/N_2 atmosphere, which contained the Pr^{3+} ions only. Within the high-temperature rhombohedral and orthorhombic phases, the $PrAlO_3$ crystals behave as simple paramagnets, whereas in the low-temperature monoclinic phase below 152 K, anomalous magnetic properties were observed. The zero-field-cooled (zfc) magnetization vs the magnetic field $M(H)$ curves exhibit nonlinear behavior in the low-field part of the virgin field sweep, whereas they become linear paramagnetic at fields larger than the "polarizing" field H_p and remain locked to the linear line for all subsequent field sweeps. The nonlinear part is absent in the field-cooled (fc) $M(H)$ curves. The zfc and fc susceptibilities exhibit very different temperature dependences as a function of the magnetic field. At low temperatures, the zfc and fc susceptibilities become temperature independent, consistent with the Van Vleck-type paramagnetism. The ^{27}Al NMR spectra show unusual tendency of increasing crystal symmetry toward cubic upon cooling. The experimental results can be explained by considering the monoclinic phase to contain tetragonally distorted domains whose fourfold axes can be reoriented by a magnetic field into the field direction. The tetragonal distortion is temperature dependent and decreases upon cooling.

DOI: 10.1103/PhysRevB.80.224410 PACS number(s): 75.60.−d, 64.70.kp, 76.60.−k

I. INTRODUCTION

Perovskites[1–13] with the general chemical formula ABO_3 represent an important class of metal oxides, having both technological and geological relevances. Physical properties of the perovskite-related oxides include colossal magnetoresistance, superconductivity, ferroelectricity and piezoelectricity, and the $MgSiO_3$ perovskite phase was found to be the dominant species in the earth's lower mantle. The high-temperature perovskite structure has cubic symmetry (space group $Pm\bar{3}m$), consisting of a framework of corner-sharing BO_6 octahedra with the A-type cation in each cuboctahedral interstice. Upon cooling, tilting of the BO_6 octahedra results in structural phase transitions to lower-symmetry phases, most commonly of the rhombohedral and orthorhombic symmetries. Among the rare-earth aluminates, $LaAlO_3$ and $NdAlO_3$ undergo a single cubic to rhombohedral ($Pm\bar{3}m \rightarrow R\bar{3}c$) structural phase transition, whereas the praseodymium aluminate[4–16] $PrAlO_3$ is special by exhibiting two additional successive structural phase transitions at lower temperatures to the orthorhombic ($Imma$) and monoclinic ($C2/m$) phases. Based on the high-resolution powder neutron and synchrotron diffraction studies of $PrAlO_3$,[8,13] the most recent view on the sequence of structural phase transitions upon cooling is $Pm\bar{3}m \rightarrow R\bar{3}c$ (~1770 K, continuous), $R\bar{3}c \rightarrow Imma$ (205 K, discontinuous), and $Imma \rightarrow C2/m$ (150 K, continuous), whereas on heating the transition temperatures were reported to be $C2/m \rightarrow Imma$ (175 K), $Imma \rightarrow R\bar{3}c$ (225 K), and $R\bar{3}c \rightarrow Pm\bar{3}m$ (~1650 K). There exists a significant scatter of the reported phase transition temperatures in literature, so that the above values should be considered as indicative. To a good approximation, all structural phase transitions in $PrAlO_3$ may be associated with the change in rotation angle of the AlO_6 octahedra about an axis in a specific (x,y,z) direction of the unit cell,[9] where the Al atom is in the center of the AlO_6 complex, O atom is common to two such complexes and rotations are in the opposite sense in adjacent unit cells. $PrAlO_3$ exhibits twinning[4] at room temperature (RT) as a result of the phase transition between the melting temperature and the room temperature, and the microtwin domain structure changes with temperature. Motion of the twin domains and boundaries with temperature and external electric and magnetic field is considered to play an important role in determining the physical properties of $PrAlO_3$. The domain structure is considered to be responsible for the hysteretic behavior of physical properties such as the magnetic susceptibility and the dielectric constant.[5] It was demonstrated that the domains at $T = 4.2$ K can be reversibly reoriented by a magnetic field with a pronounced hysteresis between the reorientation fields to the new direction and the back reorientation.[6]

Besides the richness of the structural phase transitions, $PrAlO_3$ is also interesting from the fact that structural phase transitions are coupled to the magnetic ordering of the Pr ions. $PrAlO_3$ thus belongs to the interesting class of solids with more than one instability, where the displacive and magnetic order parameters are coupled. While the structural phase transitions in $PrAlO_3$ have been extensively elaborated in the past both experimentally[4–13] and theoretically,[1–3] much less is known about the magnetic ordering. One reason could be the fact that all studies presented in literature so far were

carried out on small samples. We have not found an example of bulk single-crystal growth of this compound. Recently, we succeeded to grow large $PrAlO_3$ bulk single crystals of high structural quality by the Czochralski method.[4] Here we report a study of the unusual magnetic properties of these single-crystalline samples by performing the magnetization and magnetic susceptibility measurements and the ^{27}Al NMR spectroscopy on an as-grown sample containing a mixture of Pr^{3+} and Pr^{4+} ions and a sample annealed in a reducing H_2/N_2 atmosphere, which contained the Pr^{3+} ions only. Our study revisits and complements with new experiments the early magnetic study of $PrAlO_3$ by Cohen *et al.*,[5] dating back to 1969.

II. SAMPLES' DESCRIPTION

Details of the Czochralski-growth procedure of the $PrAlO_3$ single crystals are described in the previous publication.[4] The as-grown crystals exhibited dark brown coloration, proposed to originate from the presence of Pr^{4+} ions. Absorption spectra[4] of the as-grown samples have revealed the coexistence of Pr^{3+} and Pr^{4+} ions, where about 20% of all praseodymium ions are in the Pr^{4+} ionization state. Some as-grown crystals were annealed in a 20% H_2/N_2 reducing atmosphere at 1150 °C for 15 h, where the valence of the Pr^{4+} ions was reduced to Pr^{3+} and the coloration of the annealed samples has accordingly changed to light green, typical of Pr^{3+}-doped crystals. The annealed crystals thus contain Pr^{3+} ions only, whereas the as-grown crystals contain a Pr^{3+}/Pr^{4+} mixture at an approximate ratio 4:1. In the following, we shall refer to the two types of crystals as the "as-grown" and "annealed" samples. The lattice constants of both kinds of samples were determined by powder x-ray diffraction,[4] amounting at RT $a_h=5.3328$ Å and $c_h=12.973$ Å in hexagonal notation and $a_r=5.3083$ Å and $\alpha_r=60.305°$ in rhombohedral notation. Optical and atomic force microscopy studies[4] performed at RT have shown that all crystals possess rather periodic, ordered microtwin domains with the width of the microtwins between tens of micrometers to 100 μm. Further details of the microtwin structure at RT are given in the previous publication.[4] The samples for our measurements were cut from the parent $PrAlO_3$ crystal in the form of thin rods of dimensions $0.5 \times 0.5 \times 2$ mm^3 with the long axis parallel to the invariant twin planes.

III. EXPERIMENTAL RESULTS

A. Magnetization versus the magnetic field experiments

Magnetic measurements were conducted by a Quantum Design MPMS XL-5 superconducting quantum interference device magnetometer equipped with a 50 kOe magnet. Magnetic field was directed along the long axis of the crystals, thus parallel to the invariant twin planes. In the first set of measurements, the magnetization M versus the magnetic field H curves were measured in fields up to 50 kOe at a set of temperatures between 300 and 5 K, chosen to include all the investigated phases—the rhombohedral, orthorhombic, and monoclinic. The samples were cooled to a selected temperature in zero magnetic field by always starting the cooling run at 300 K. This type of $M(H)$ curves is referred in the following as the zero-field-cooled (zfc) $M(H)$ curves. The zfc $M(H)$ curves of the annealed sample are shown in Fig. 1, whereas those of the as-grown sample are shown in Fig. 2. For both samples, the following features are observed. At the temperatures between 300 and 152 K, corresponding to the rhombohedral and orthorhombic phases, the $M(H)$ curves are linear paramagnetic with no hysteresis within the investigated field sweep ± 50 kOe. After crossing the transition temperature of 152 K to the monoclinic phase, the zfc $M(H)$ curves behave differently. Starting the field sweep from $H=0$, the "virgin" part of the zfc $M(H)$ curve exhibits nonlinear behavior in the low-field regime, showing irregular growth with increasing H and exhibiting kinks. At a sufficiently large H (denoted as the "polarizing" field H_p), the virgin curve becomes linear paramagnetic, the growth with H becomes stronger, and the magnetization remains locked to the linear line for all subsequent up-down $M(H)$ runs. The part of the $M(H)$ curve for positive H at the temperature 5 K is displayed in the insets of Figs. 1 and 2 for the annealed and the as-grown sample, respectively, where H_p is indicated by a dashed line. H_p exhibits quite strong temperature dependence. At $T=125$ K, the field of 50 kOe is just enough to drive the $M(H)$ curves into the linear regime, whereas at lower temperatures, the polarizing field becomes progressively smaller, amounting at 5 K about 35 kOe for the annealed sample and 20 kOe for the as-grown sample. There thus exists significant difference in the magnitude of the polarizing field between the annealed and the as-grown

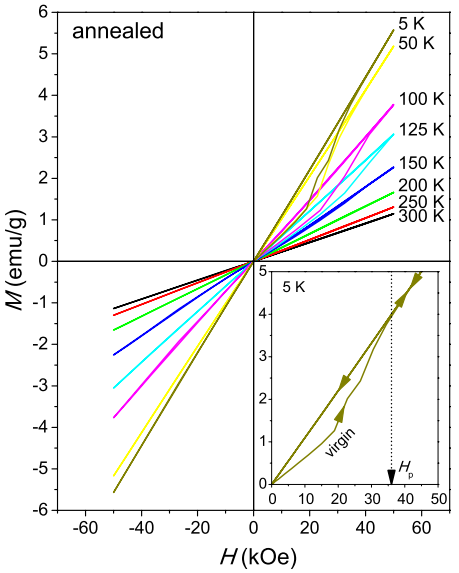

FIG. 1. (Color online) zfc $M(H)$ curves of the annealed $PrAlO_3$ sample. The inset shows the zfc $M(H)$ curve at $T=5$ K, where virgin denotes the nonlinear part of the curve in the initial field sweep after the crystal was cooled in zero magnetic field. The polarizing field H_p is marked by an arrow on the field axis and the arrows on the $M(H)$ curve show the direction of the magnetization change during the field sweep. Once polarized in the field $H>H_p$, the magnetization remains locked to the linear line for all subsequent field sweeps.

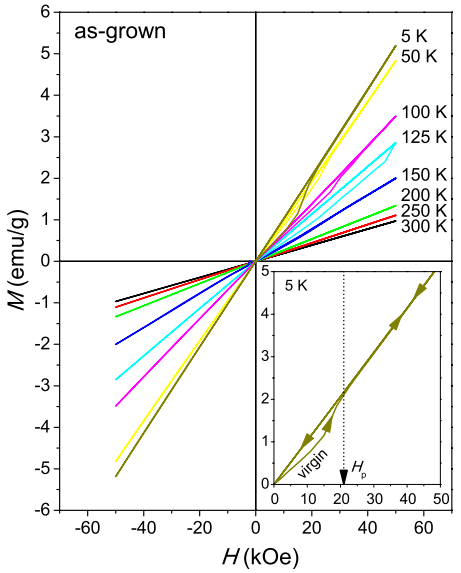

FIG. 2. (Color online) zfc $M(H)$ curves of the as-grown $PrAlO_3$ sample. The inset shows the zfc $M(H)$ curve at $T=5$ K, where virgin denotes the nonlinear part of the curve in the initial field sweep after the crystal was cooled in zero magnetic field. The polarizing field H_p is marked by an arrow on the field axis and the arrows on the $M(H)$ curve show the direction of the magnetization change during the field sweep. Once polarized in the field $H>H_p$, the magnetization remains locked to the linear line for all subsequent field sweeps.

samples, where the as-grown sample generally exhibits smaller H_p.

In order to further elucidate the properties of the nonlinear virgin part of the zfc $M(H)$ curves, the $M(H)$ experiments were repeated under the field-cooled (fc) condition by applying the field of 50 kOe at RT and then cooling in this field down to the measurement temperature of 5 K. The corresponding magnetization curve is denoted as the fc $M(H)$ curve. The fc $M(H)$ curves at $T=5$ K of the annealed and the as-grown samples are shown in Fig. 3. For both samples, the fc $M(H)$ curves are strictly linear and the nonlinear part observed in the virgin zfc $M(H)$ curves of Figs. 1 and 2 is absent.

The above $M(H)$ experiments reveal that within the two high-temperature phases—the rhombohedral and the

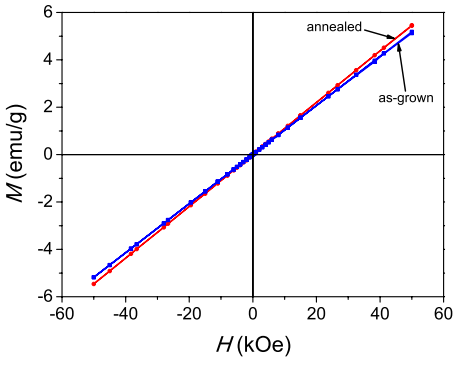

FIG. 3. (Color online) fc $M(H)$ curves of the as-grown and annealed $PrAlO_3$ samples at $T=5$ K after cooling the samples in the field of 50 kOe.

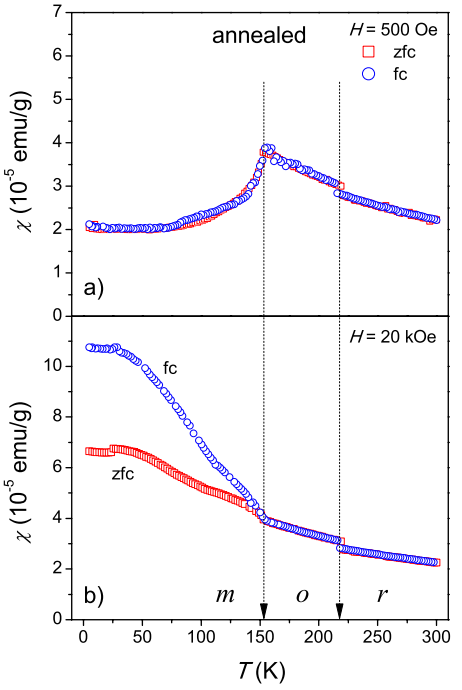

FIG. 4. (Color online) Temperature-dependent zfc and fc magnetic susceptibilities of the annealed $PrAlO_3$ sample in (a) low magnetic field of 500 Oe and (b) high magnetic field of 20 kOe. The phases are denoted r for rhombohedral, o for orthorhombic, and m for monoclinic.

orthorhombic—the system of Pr spins behaves as a simple paramagnet with a linear $M(H)$ relation within the investigated magnetic field sweep of ± 50 kOe, whereas in the low-temperature monoclinic phase below 152 K, the behavior is changed. The virgin zfc $M(H)$ curve behaves nonlinear in the low-field regime, but can be driven into a linear $M(H)$ regime by a sufficiently strong external magnetic field $H>H_p$, indicating a kind of magnetic field induced structural rearrangement and/or domain polarization.

B. zfc and fc magnetic susceptibility

The zfc and fc dc magnetic susceptibilities $\chi=M/H$ were measured between 300 and 2 K in magnetic fields of 500 Oe and 20 kOe. The crystals were first cooled in zero field to 2 K, where the field was applied and χ_{zfc} was subsequently measured in a heating run. After 300 K was reached, the temperature sweep was reversed and χ_{fc} was measured in a cooling run. The zfc and fc susceptibilities of the annealed sample in $H=500$ Oe are displayed in Fig. 4(a). χ_{zfc} and χ_{fc} are practically identical ($\chi_{zfc}\approx\chi_{fc}$) in the entire investigated temperature range. Within the high-temperature rhombohedral and orthorhombic phases, χ_{zfc} and χ_{fc} show a paramagnetic growth upon cooling. At the rhombohedral-to-orthorhombic first-order transition, χ_{zfc} and χ_{fc} both exhibit a small discontinuous jump to a higher value. The jump occurs at the temperature of about 220 K with an up-down hysteresis of $\Delta T\approx 5$ K. Below the orthorhombic-to-monoclinic second-order phase transition at 152 K, the temperature trend of χ_{zfc} and χ_{fc} is reversed. The susceptibilities start to de-

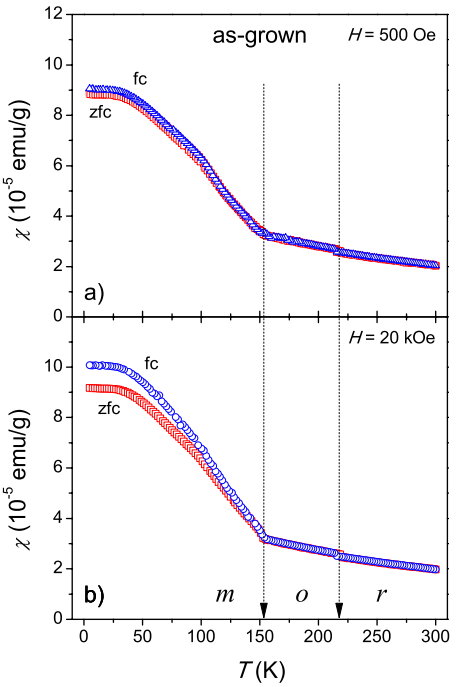

FIG. 5. (Color online) Temperature-dependent zfc and fc magnetic susceptibilities of the as-grown $PrAlO_3$ sample in (a) low magnetic field of 500 Oe and (b) high magnetic field of 20 kOe. The phases are denoted *r* for rhombohedral, *o* for orthorhombic, and *m* for monoclinic.

crease and saturate to a temperature-independent plateau below 80 K. The zfc and fc susceptibilities in a higher field of 20 kOe are displayed in Fig. 4(b). While in the high-temperature rhombohedral and orthorhombic phases, the susceptibilities are basically unchanged with respect to the low-field case, the higher magnetic field of 20 kOe has drastically changed the susceptibilities within the low-temperature monoclinic phase. At the orthorhombic-to-monoclinic transition at 152 K, both susceptibilities exhibit a kink, whereas below 152 K, χ_{zfc} and χ_{fc} become unequal ($\chi_{zfc} < \chi_{fc}$) and their temperature trend is reversed with respect to the low-field case. χ_{fc} increases rapidly upon cooling and levels off to a temperature-independent plateau below 30 K. χ_{zfc} behaves similarly, but its value is considerably smaller than χ_{fc}. Comparing the magnitudes of the high field and low field χ_{fc} (which in the low field equals χ_{zfc}) at the lowest investigated temperature of 2 K, we find $\chi_{fc}^{20\ kOe}/\chi_{fc}^{500\ Oe} \approx 5$.

The temperature-dependent χ_{zfc} and χ_{fc} of the as-grown sample in the low magnetic field of 500 Oe are displayed in Fig. 5(a). Within the rhombohedral and orthorhombic phases, χ_{zfc} and χ_{fc} are again equal and exhibit paramagnetic increase with decreasing temperature, but the discontinuous jump at the rhombohedral-to-orthorhombic transition at about 220 K is smaller and less pronounced as compared to the annealed sample. At the orthorhombic-to-monoclinic transition at 152 K, both susceptibilities again exhibit a kink, whereas below 152 K χ_{zfc} and χ_{fc} increase rapidly and level off to a temperature-independent plateau below about 30 K. Within the low-temperature monoclinic phase, χ_{zfc} and χ_{fc} are almost equal in the low field; $\chi_{zfc} \approx \chi_{fc}$. Repeating the measurements in the high magnetic field of 20 kOe [Fig. 5(b)], χ_{zfc} and χ_{fc} are basically unchanged with respect to the low-field case, except that the inequality $\chi_{zfc} < \chi_{fc}$ is now observed.

The above measurements of χ_{zfc} and χ_{fc} demonstrate the strong influence of the magnetic field on the magnetic susceptibility within the low-temperature monoclinic phase, in agreement with the $M(H)$ experiments presented in Figs. 1–3. In contrast, the magnitude of the magnetic field plays no measurable role on the magnetic susceptibility within the two high-temperature phases above 152 K. The discussion of this phenomenon will be given after the susceptibility and $M(H)$ experiments are complemented by the ^{27}Al NMR measurements, to be presented next.

C. ^{27}Al NMR spectra

The measurements of the temperature-dependent ^{27}Al NMR spectra were performed in a magnetic field $H_0 = 47$ kOe at temperatures between 300 and 80 K in both cooling and heating runs, by starting at 300 K and cooling to 80 K, where the temperature sweep was reversed and the spectra were subsequently measured in a heating run. For most of the investigated temperature interval, the measurements were performed in steps $\Delta T = 5$ K, whereas around the phase transition to the monoclinic phase at 152 K, the spectra were recorded every $\Delta T = 1$ K. It is important to emphasize that our NMR experiments performed in the magnetic field of 47 kOe correspond to the field-cooled case, where the related fc $M(H)$ curves of Fig. 3 are strictly linear.

The ^{27}Al nucleus possesses spin $I = 5/2$ and interacts with the surrounding electric charges via the electric quadrupole interaction. In the $PrAlO_3$ structure, Al atoms are located at the center of the AlO_6 octahedra, so that the closest charges of an Al atom are six oxygen atoms in the corners of the octahedron. Upon changing the temperature, the ^{27}Al nuclei sense redistribution of the nearest oxygens (due to distortions and rotations of the AlO_6 octahedra) and the Pr atoms via the changes in the electric field gradient (EFG) tensor that these atoms produce at the octahedron center. The temperature-dependent ^{27}Al spectra were recorded at a general orientation of the crystals in the magnetic field, where none of the crystallographic axes was parallel to the field. For the crystal symmetry lower than cubic, the ^{27}Al NMR spectrum consists of five lines, a central line ($1/2 \leftrightarrow -1/2$ transition) that is quadrupole perturbed in second order and two pairs of satellites, quadrupole perturbed in first order. Twinning of the structure may produce additional splitting of each line in the spectrum for twin domains that are not parallel or antiparallel to each other.

The ^{27}Al NMR spectra of the as-grown sample in the rhombohedral, orthorhombic, and monoclinic phases in a cooling run are shown in Fig. 6(a), whereas the temperature-dependent peak positions are displayed in Figs. 7(a) and 7(b) for the cooling and heating runs, respectively. The origin of the frequency axis was taken at the ^{27}Al resonance of the $AlCl_3$ aqueous solution. In the high-temperature rhombohedral phase, we observe the expected multiplet of five lines, where the outer satellites are additionally split into doublets [marked by arrows on the 290 K spectrum in Fig. 6(a)] that

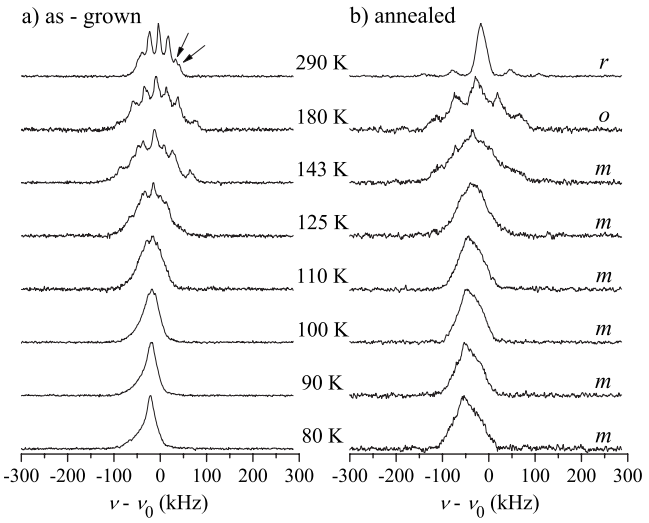

FIG. 6. Selected ^{27}Al NMR spectra in a cooling run of (a) the as-grown $PrAlO_3$ crystal and (b) the annealed crystal in the magnetic field of 47 kOe. Orientations of the crystals in the magnetic field are not the same. The symbol *r* denotes the rhombohedral phase, *o* the orthorhombic, and *m* the monoclinic. The arrows on the 290 K spectrum of the as-grown sample indicate the additional splitting of the outer satellite line due to the presence of slightly nonparallel twin domains at RT.

can be associated with slightly nonparallel twin domains. The inner satellites are just broadened by this domain structure, but resolved peaks are not observed. The peak positions of the ^{27}Al multiplet do not change with temperature within

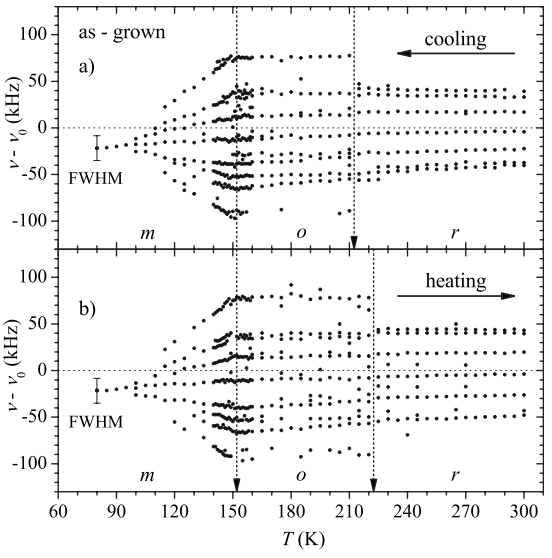

FIG. 7. Temperature-dependent peak positions of the lines in the ^{27}Al quadrupole-perturbed spectrum of the as-grown $PrAlO_3$ crystal for (a) the cooling run and (b) the heating run. The origin of the frequency axis was taken at the ^{27}Al resonance frequency ν_0 of the $AlCl_3$ aqueous solution. Dashed vertical lines with arrows denote approximate transition temperatures between the rhombohedral (*r*), orthorhombic (*o*), and monoclinic (*m*) phases. The bar on the point at the lowest measuring temperature of 80 K denotes the full width at half maximum of the residual line after the multiplet spectrum collapse.

the rhombohedral phase, demonstrating that the EFGs at the ^{27}Al sites are constant and no temperature-dependent rearrangement of the atoms takes place. At the rhombohedral-to-orthorhombic discontinuous phase transition, the structure of the ^{27}Al spectrum undergoes an abrupt change. The multiplicity of lines is increased, suggesting the appearance of a different domain structure in the orthorhombic phase. Apart from this sudden change in the NMR spectrum, the peak positions of the ^{27}Al multiplet do not show further changes with temperature within the orthorhombic phase, demonstrating that the EFGs are constant and no further temperature-dependent rearrangements of the atoms take place within that phase. At the orthorhombic-to-monoclinic transition at 152 K, the structure of the spectrum starts to change continuously. The splitting between the lines starts to diminish until at about 95 K, all lines collapse onto a single line. This indicates a tendency of gradual *increase* in the Al site symmetry toward cubic, in which case the EFG vanishes and the ^{27}Al NMR spectrum consists of a single line at the nuclear Larmor frequency instead of five quadrupole-perturbed lines. The single line continues to narrow upon further cooling [Fig. 6(a)], but its width at the lowest investigated temperature of 80 K is still relatively broad [the full width at half maximum amounts about 50 kHz and is shown by a bar in Figs. 7(a) and 7(b)], indicating that the exact Al site symmetry may not be cubic but pseudocubic only, where the departure from the true cubic symmetry is large enough to broaden the line but insufficient to yield resolved lines in the spectrum. Repeating the ^{27}Al NMR experiment in a heating run [Fig. 7(b)] by starting the heating run immediately after the cooling run was completed, thus after a field-cooled experiment, the spectrum behaves practically identically as in the preceding cooling run. The temperature-dependent NMR spectrum collapse phenomenon in the monoclinic phase is thus fully reversible. It is worth mentioning that the orthorhombic-to-monoclinic continuous transition is observed at the same temperature 152 K in both cooling and heating runs, whereas an up-down hysteresis in the transition temperature of about $\Delta T \approx 10$ K is observed for the discontinuous rhombohedral-to-orthorhombic transition.

The ^{27}Al NMR experiment was repeated on the annealed sample and the spectra in a cooling run are displayed in Fig. 6(b), whereas the temperature-dependent peak positions for the cooling and heating runs are displayed in Figs. 8(a) and 8(b). The slightly different structure of the spectrum of the annealed sample, as compared to that of the as-grown sample from Fig. 7 is due to different orientation of the crystal in the magnetic field. The temperature-dependent vanishing of the quadrupolar splitting between the lines of the ^{27}Al spectrum upon cooling is again observed in the monoclinic phase. The full width at half maximum of the residual line at 80 K after the spectrum collapse remains relatively large, amounting about 75 kHz (shown by a bar in Fig. 8), indicating again a pseudocubic rather than a true cubic symmetry at low temperatures. The equality of the spectra in the cooling and heating runs also indicates that the collapse phenomenon is reversible.

IV. DISCUSSION

The above-presented magnetic and NMR results show unusual features in the low-temperature monoclinic phase. An

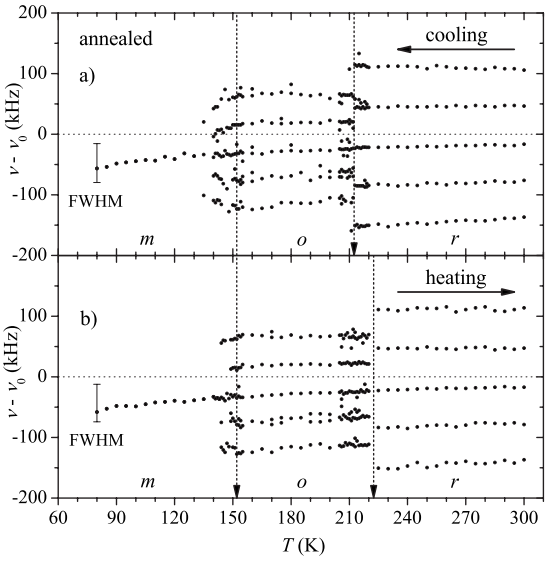

FIG. 8. Temperature-dependent peak positions of the lines in the ^{27}Al quadrupole-perturbed spectrum of the annealed $PrAlO_3$ crystal for (a) the cooling run and (b) the heating run. Other details are the same as in Fig. 7.

explanation can be given in terms of the distortion of the $PrAlO_3$ crystal structure under the combined influence of temperature and magnetic field. Optical spectroscopy experiments[5,6] have shown that the approximate Pr^{3+} site symmetry in the monoclinic phase is cubic with a small tetragonal distortion. A macroscopic $PrAlO_3$ crystal consists of tetragonal domains whose fourfold axes are oriented along the cubic axes of the perovskite structure and can be reoriented by a magnetic field. The $M(H)$ and magnetic susceptibility experiments can readily be explained by adopting the following physical picture: (i) within the monoclinic phase, a sufficiently large external magnetic field distorts the crystalline structure in a way that the fourfold axis of the tetragonal domains is rotated into the direction of the magnetic field; (ii) the tetragonal distortion is temperature dependent and decreases upon cooling; (iii) the smaller the tetragonal distortion, the smaller is the magnetic field needed to reorient the domains; and (iv) the magnetization of a domain oriented with its tetragonal axis along the field is a factor about five larger than for the perpendicular orientation. The zfc and fc $M(H)$ experiments presented in Figs. 1–3 can be explained by the above assumptions. In a zfc $M(H)$ experiment, the crystal is cooled in the absence of a magnetic field. During zfc cooling, the tetragonal domains orient into an energetically favorable configuration along all possible cubic perovskite directions to minimize the crystalline free energy. Applying the field sweep of the $M(H)$ experiment, the perpendicular domains start to reorient into the field in order to minimize the paramagnetic free energy, giving the irregularly growing part of the virgin zfc $M(H)$ curves. Since the magnetization of the perpendicular domains is smaller from that of the parallel domains, the total magnetization of the sample in the virgin $M(H)$ run is initially smaller than it would be for the case when all the domains would be parallel to the field. Increasing the field strength, the volume of the parallel domain increases at the expense of the perpendicular domains and full polarization is obtained for the field larger than the polarizing field H_p. For $H > H_p$, the crystal is single domain and remains locked to this state for all subsequent $M(H)$ runs. Once polarized in the field $H > H_p$, the $M(H)$ curves remain linear paramagnetic, representing the temperature-independent Van Vleck paramagnetism at low temperatures, to be discussed later. In the fc $M(H)$ experiments of Fig. 3, where the cooling was performed in a high magnetic field of 50 kOe, the tetragonal domains were reoriented into the field already during the cool down, so that the fc $M(H)$ curves are linear paramagnetic in the entire field sweep range without the irregular nonlinear part observed in the virgin zfc $M(H)$ curves for $H < H_p$. The fact that the polarizing field H_p decreases upon lowering the temperature can be explained on the basis of the ^{27}Al NMR spectra, where the collapse of the quadrupolar lines onto a single line upon cooling demonstrates that the tetragonal distortion decreases and the symmetry is virtually increased toward cubic. Adopting that the domains with smaller tetragonal distortion are reoriented by a smaller magnetic field explains the observed decrease in the polarizing field H_p upon cooling. Here it is also worth mentioning that there is no qualitative difference between the $M(H)$ experiments of the annealed and as-grown samples, whereas there exists quantitative difference in the magnitude of the polarizing field H_p that is generally larger for the annealed sample (recall that at 5 K, $H_p \approx 35$ kOe for the annealed sample, whereas $H_p \approx 20$ kOe for the as-grown sample). This difference can be partly attributed to the details of the domain structure in the two samples that is a sensitive function of the sample growth conditions, cooling history, the amount of impurities and the external strain. The influence of the Pr valence state (Pr^{3+} for the annealed sample and a Pr^{3+}/Pr^{4+} mixture for the as-grown sample) is not clear, but may add to this difference as well.

The same physical picture explains the temperature-dependent zfc and fc magnetic susceptibilities in the low and high magnetic fields, presented in Figs. 4 and 5. We consider first the susceptibility of the annealed sample in the low-temperature monoclinic phase. In the low-field experiment [Fig. 4(a)], the magnetic field $H=500$ Oe is insufficient to reorient the tetragonal domains for both the zfc and fc cooling protocols. In both cases, the domains orient into an energetically favorable configuration along all possible cubic perovskite directions in order to minimize the crystalline free energy, which wins over the paramagnetic free energy. Consequently we have $\chi_{zfc} \approx \chi_{fc}$ and the susceptibility values are small, representing an average over the distribution of parallel and perpendicular domains. The temperature dependence of χ_{zfc} and χ_{fc} will be discussed later by considering the energy levels of a Pr^{3+} ion in the crystalline electric field, but their temperature independence below 80 K is again in favor of the Van Vleck paramagnetism at low temperatures. In the high-field experiment [Fig. 4(b)], the magnetic field $H=20$ kOe is according to the $M(H)$ results of Fig. 1 already strong enough to partially reorient the domains into the field, so that the paramagnetic free energy starts to dominate over the crystalline free energy. The continuously growing χ_{zfc} and χ_{fc} upon cooling within the monoclinic phase and their considerably larger values as compared to the low-field case

are a consequence of the gradual domain reorientation into the field direction (as discussed above, progressively smaller magnetic fields are needed for the reorientations at lower temperatures, which results in a gradual buildup of the magnetization upon cooling), and the fact that the volume of the parallel domain with higher susceptibility increases at the expense of the perpendicular domains, whose susceptibility is lower. At temperatures below about 30 K, the high-field χ_{zfc} and χ_{fc} saturate to a temperature-independent plateau compatible with the Van Vleck paramagnetism. Here it is worth mentioning that the employed field of 20 kOe represents for the annealed sample an intermediate case between the nonpolarized domains in low field and fully polarized domains at fields $H > H_p$, which is at the origin of the remnant behavior $\chi_{zfc} < \chi_{fc}$.

The zfc and fc susceptibilities of the as-grown sample conform to the same physical picture, except that the domains in the monoclinic phase appear "softer" to reorient into the field, in agreement with the smaller polarizing field H_p of this sample, as compared to the annealed one. This indicates differences in the domain structure between the two samples due to uncontrolled details in the sample growth conditions, cooling history, impurities, and external strain. The influence of the Pr^{3+}/Pr^{4+} mixture to this effect in the as-grown sample is again not clear, but may play a role as well as the Pr^{4+} energy levels in the crystalline electric field are different from those of the Pr^{3+} ion and the Pr^{4+} fraction is significant (about 20%). In the monoclinic phase, there is again practically no difference between χ_{zfc} and χ_{fc} in the low field of 500 Oe, whereas they become slightly unequal in the high field of 20 kOe. The fact that the remanence $\chi_{zfc} < \chi_{fc}$ of the as-grown sample in 20 kOe is considerably smaller than that of the annealed sample under the same experimental condition can be attributed to the smaller polarizing field of the as-grown sample. For $H > H_p$, all the domains are parallel to the field (i.e., the crystal becomes single domain) and no remanence is expected any more, so that the equality $\chi_{zfc} \approx \chi_{fc}$ should be fulfilled again. For the as-grown sample, the applied field of 20 kOe is close to the H_p value at 5 K of this sample and the domain remanence is largely lost in this field, whereas for the annealed sample, the applied field is only about half of $H_p \approx 35$ kOe at 5 K of that sample, which is not strong enough to fully polarize the domains. Consequently, the remanent case $\chi_{zfc} < \chi_{fc}$ is observed for the annealed sample in Fig. 4(b) at this intermediate applied field, whereas the remanence of the as-grown sample is considerably smaller in the same field [Fig. 5(b)].

We return now to the temperature dependence of the magnetic susceptibility of $PrAlO_3$. The case already elaborated in literature on the basis of optical spectroscopy is the one for the crystal containing only the Pr^{3+} ions, which is applicable to our annealed sample. The temperature-dependent susceptibility for this case was explained in terms of the temperature-dependent Pr^{3+} energy levels in the crystalline electric field. According to Cohen *et al.*,[5] the three lowest Stark levels of the ground multiplet $^3H_4$ of Pr^{3+} are singlets. In the high-temperature rhombohedral and orthorhombic phases, where several of the Stark components are populated, the crystal behaves like a simple paramagnet. At low temperatures, the only contribution to the magnetization is due to the second-order-induced magnetization of the low-lying singlets, corresponding to Van Vleck temperature-independent paramagnetism. The temperature dependence of the susceptibility in the monoclinic phase below 152 K can be ascribed to the variation in separation between the singlet levels as a function of temperature. As observed in Fig. 4(a), the limit of the temperature-independent Van Vleck susceptibility in the low field is reached below 80 K. The linear paramagnetic $M(H)$ curves of Figs. 1 and 3 (except for the virgin part of the zfc curves in the monoclinic phase, where the domains are still orienting into the field) support the above physical picture. Qualitatively similar results on the temperature-dependent $^3H_4$ ground multiplet levels of Pr^{3+}, but showing quantitative differences, were also reported by Harley *et al.*[9] on the basis of fluorescence spectrum of $PrAlO_3$. Application of the above Pr^{3+} energy-level scheme[5,9] to our as-grown sample that contains a Pr^{3+}/Pr^{4+} mixture is not straightforward and we skip the discussion.

In the final step, we discuss the ^{27}Al NMR results and demonstrate that the collapse of the ^{27}Al quadrupole-perturbed multiplet spectrum onto a single line upon cooling within the monoclinic phase originates from the temperature-dependent decrease in the tetragonal distortion and not from the rotation of the fourfold axis of tetragonal domains into the direction of the magnetic field. The EFG tensor generally shows the symmetry equivalent to the site symmetry of the resonant nucleus. For the tetragonal site symmetry, the ^{27}Al EFG tensor is diagonal in the crystal-fixed frame. Assuming that the tetragonal axis points along the z crystallographic direction, the diagonal elements of the EFG tensor are $V_{zz} = eq$ and $V_{xx} = V_{yy} = -eq/2$. In the first-order perturbation, the corresponding quadrupole-perturbed spectrum shows a multiplet structure of five lines with the central line located at the Larmor frequency, whereas the four satellites are displaced from the Larmor frequency by $\pm\nu_Q$ and $\pm 2\nu_Q$ (where $\nu_Q = 3e^2qQ/20h$ is the ^{27}Al quadrupole coupling constant). This multiplet structure is retained even when the domains are fully aligned with the magnetic field. For a cubic site symmetry, the EFG tensor should again be diagonal in the crystal-fixed frame, this time with all three elements equal by symmetry requirements: $V_{xx} = V_{yy} = V_{zz}$. Since the diagonal elements are related by the Laplace equation $V_{xx} + V_{yy} + V_{zz} = 0$, this requires that all three elements are zero and the corresponding spectrum consists of a single line at the Larmor frequency. The observed collapse of the ^{27}Al five-line multiplet upon cooling within the monoclinic phase thus reflects the temperature-dependent decrease in the tetragonal distortion and is hence an effect of temperature with no direct relationship to the magnetic field and the associated rotation of the domains into the field direction. This is supported by the neutron diffraction structural study performed in zero magnetic field,[7] where a decrease in the tetragonal distortion toward lower temperatures in the monoclinic phase was observed as well.

V. CONCLUSIONS

We have investigated unusual magnetism of the $PrAlO_3$ perovskite system by performing measurements of the mag-

netization, magnetic susceptibility, and ^{27}Al NMR spectra on single crystals, prepared by the Czochralski method. Our experimental results can be consistently explained by the physical picture that considers the monoclinic phase of the $PrAlO_3$ crystal to consist of tetragonal domains whose fourfold axes are oriented along the cubic axes of the perovskite structure and can be reoriented by a magnetic field. A sufficiently large external magnetic field distorts the crystalline structure in a way that the fourfold axis of the tetragonal domains is rotated into the direction of the magnetic field. The tetragonal distortion is temperature dependent and decreases upon cooling. The smaller is the tetragonal distortion, the smaller is the magnetic field needed to reorient the domains. The observed collapse of the ^{27}Al quadrupole-perturbed multiplet upon cooling within the monoclinic phase reflects the temperature-dependent decrease in the tetragonal distortion. It is an effect of temperature with no direct relationship to the magnetic field and the associated rotation of the domains into the field direction. The origin of the distortion of the $PrAlO_3$ structure in the magnetic field is the extremely small anisotropy in the crystalline free energy that can be overcome by the anisotropy in the paramagnetic free energy.

ACKNOWLEDGMENTS

S.T. and D.A.P. thank the Ministry of Scientific Research and Information Technology of Poland and the FP7 NMP ENSEMBLE Project (Grant No. GA NMP4-SL-2008-213669) for support.

*On leave from Institute of Molecular Physics, Polish Academy of Sciences, Smoluchowskiego 17, 60-179 Poznań, Poland.

[1] P. M. Woodward, Acta Crystallogr., Sect. B: Struct. Sci. **53**, 32 (1997).
[2] C. N. W. Darlington, Phys. Status Solidi B **203**, 73 (1997).
[3] C. J. Howard and H. T. Stokes, Acta Crystallogr., Sect. B: Struct. Sci. **54**, 782 (1998).
[4] D. A. Pawlak, T. Lukasiewicz, M. Carpenter, M. Malinowski, R. Diduszko, and J. Kisielewski, J. Cryst. Growth **282**, 260 (2005).
[5] E. Cohen, L. A. Risberg, W. A. Nordland, R. D. Burbank, R. C. Sherwood, and L. G. Van Uitert, Phys. Rev. **186**, 476 (1969).
[6] L. A. Riseberg, E. Cohen, W. A. Nordland, and L. G. Van Uitert, Phys. Lett. **30A**, 4 (1969).
[7] M. A. Carpenter, C. J. Howard, B. J. Kennedy, and K. S. Knight, Phys. Rev. B **72**, 024118 (2005).
[8] S. M. Moussa, B. J. Kennedy, B. A. Hunter, C. J. Howard, and T. Vogt, J. Phys.: Condens. Matter **13**, L203 (2001).
[9] R. T. Harley, W. Hayes, A. M. Perry, and S. R. P. Smith, J. Phys. C **6**, 2382 (1973).
[10] B. J. Kennedy, T. Vogt, C. D. Martin, J. B. Parise, and J. A. Hriljac, Chem. Mater. **14**, 2644 (2002).
[11] R. D. Burbank, J. Appl. Crystallogr. **3**, 112 (1970).
[12] P. A. Fleury, P. D. Lazay, and L. G. Van Uitert, Phys. Rev. Lett. **33**, 492 (1974).
[13] B. J. Kennedy, A. K. Prodjostanoso, and C. J. Howard, J. Phys.: Condens. Matter **11**, 6319 (1999).
[14] R. J. Birgeneau, J. K. Kjems, G. Shirane, and L. G. Van Uitert, Phys. Rev. B **10**, 2512 (1974).
[15] K. B. Lyons, R. J. Birgeneau, E. I. Blount, and L. G. Van Uitert, Phys. Rev. B **11**, 891 (1975).
[16] J. K. Kjems, G. Shirane, R. J. Birgeneau, and L. G. Van Uitert, Phys. Rev. Lett. **31**, 1300 (1973).